Journal on Oncology

www.journalononcology.org

Research Article

Open Access, Volume 3

Monitoring the Time-Dependent Effects of Prostate Brachy- and Radiotherapy

Weis Jan[1]*; Johansson Adam[1]; Jafar Maysam[2]; Dahlman Pär[3#]; Taheri-Kadkhoda Zahra[4#]

[1]Department of Medical Physics, University Hospital, Uppsala, Sweden.

[2]Philips Nordic, Stockholm, Sweden.

[3]Section of Radiology, Department of Surgical Sciences, University Hospital, Uppsala, Sweden.

[4]Department of Oncology, University Hospital, Uppsala, Sweden.

[#]These Authors Contributed Equally to this Work.

Abstract

External beam radiotherapy (EBRT), brachytherapy (BT), and a combination of BT with EBRT are among common treatments for localized prostate cancer. Published studies reveal variations in treatment approaches, both in total radiation dose delivered to the prostate and in efficiency of the treatment. Therefore, assessment of prostate response to radiotherapy (RT) is still important subject of the research. The purpose of this work was assessment of prostate metabolic activity using single-voxel MR spectroscopy (MRS) and evaluation of apparent diffusion coefficients (ADC) before, during and three months after the completion of BT and/or EBRT. The second aim was to investigate both methods in assessing the response of prostate tissues to RT. Seven patients underwent either BT combined with EBRT or only EBRT delivered by 1.5T MR-Linac. MR examinations were performed on a 3T scanner. Single-voxel MRS was performed with point-resolved spectroscopy. Prostate metabolites and ADC were quantified before, during, and three months after the end of therapy. Polyamines (PA) and citrate (Cit) intensities decreased significantly after BT. Cit intensity decreased almost to the noise level three months after the end of EBRT. The spectral intensity ratio Cit/(Cho+PA+Cr) was found to be a good indicator of the biochemical response of prostate tissue to RT. BT caused rapid decrease of ADC values followed by an increase. ADC values of patients treated only by EBRT increased during therapy. Single-voxel MRS was found to be a useful tool in monitoring metabolic response of the prostate during and after BT or EBRT. Good biochemical response to radiotherapy can be characterized by a low Cit intensity and by an increase in ADC values. Spectroscopic data of prostate metabolic activity may provide important predictive information following radiotherapy.

Keywords: Prostate cancer; Brachytherapy; Radiotherapy; MR-Linac; MRS; ADC; Response to therapy.

Abbreviations: EBRT: External Beam Radiotherapy; BT: Brachytherapy; RT: Radiotherapy; MR: Magnetic Resonance; MRS: MR Spectroscopy; ADC: Apparent Diffusion Coefficient; Cit: Citrate; Cr: Creatine; Cho: Choline; PA: Polyamines; PCa: Prostate Cancer; PSA: Prostate Specific Antigen; DWI: Diffusion Weighted Imaging; MRSI: MR Spectroscopic Imaging; MA: Metabolic Atrophy; SNR: Signal to Noise Ratio; TR: Time Repetition; TE: Time Echo; SENSE: Sensitivity Encoding; FOV: Field of View; IMRT: Intensity Modulated Radiotherapy; NSA: Number of Signal Averages; SE: Spin Echo; EPI: Echo Planar Imaging; SPAIR: Spectrally Selective Attenuated Inversion Recovery; PRESS: Point Resolved Spectroscopy; BASING: Band Selective Inversion with Gradient Dephasing; ADT: Androgen Deprivation Therapy; LCModel: Linear Combination of Model Spectra; CRLB: Cramér-Rao Lower Bound.

Manuscript Information: *Received: Sep 13, 2023; Accepted: Oct 09, 2023; Published: Oct 16, 2023*

Correspondance: *Jan Weis, Department of Medical Physics, Uppsala University Hospital, SE-751 85 Uppsala, Sweden.*

Email: jan.weis@radiol.uu.se

Citation: *Jan W, Adam J, Maysam J, Pär D, Zahra TK. Monitoring the Time-Dependent Effects of Prostate Brachy- and Radiotherapy. J Oncology. 2023; 3(2): 1108.*

Introduction

External beam radiotherapy (EBRT), brachytherapy (BT), and a combination of BT with EBRT are among common treatments for clinically localized low- to intermediate-risk prostate cancer (PCa) [1-3]. Radical prostatectomy, androgen deprivation therapy and cryoablation are alternative treatment options for this localized disease [4]. Published studies reveal variations in treatment approaches, both in total radiation dose delivered to the prostate and in efficiency of the treatment [5-8]. Therefore, assessment of prostate response to radiotherapy (RT) is still investigational pending long-term prospective comparative data [9].

Response to RT is routinely evaluated by assessing changes in prostate-specific antigen (PSA) levels in serum before and after RT. After therapy, PSA levels can transiently increase (the so-called PSA bounce phenomenon) before dropping below the nadir values before intervention [10]. Biochemical failure after RT occurs in 30-50% of the patients [11,12]. This failure initiates further examinations with the aim to confirm or exclude PCa recurrence. Transrectal ultrasound-guided sextant biopsy is the current standard for histological verification of local PCa recurrence [13]. This is an invasive approach and can be inaccurate in the depiction of some tumors as only a fraction of the prostate gland is sampled.

Magnetic resonance imaging (MRI) and proton (^{1}H) magnetic resonance spectroscopy (^{1}H-MRS) are frequently used as complementary approaches to ultrasound-guided sextant biopsy for the detection and localization of PCa before and after RT. Whilst standard T_2-weighted MR imaging is useful for anatomical detection and localization of suspicious lesions before RT, its ability to identify PCa post-therapy is considerably limited due to loss of zonal anatomy and diffuse reduction of T_2-weighted signal caused by therapy-induced glandular atrophy and fibrosis [5,6,13]. Currently, diffusion weighted imaging (DWI) is frequently used in addition to T_2-weighted sequences both for diagnostic and surveillance purposes. The apparent diffusion coefficient (ADC) maps derived from DWI, when used as an adjunct to weighted images, have been shown to be invaluable for identifying recurrent PCa lesions larger than 0.4 cm^2 [14]. Furthermore, 3D magnetic resonance spectroscopic imaging (3D MRSI) improves detection and localization of PCa before therapy and has shown good potential to recognize residual and recurrent PCa after therapy [5,6,8,13]. 3D MRSI may confirm successful radiation treatment by identifying metabolic atrophy (MA) that reflects decrease and/or loss of prostatic metabolites [5,6,15-17]. Prostatic metabolites that MR spectroscopy can detect and quantify are total choline (Cho), polyamines (PA) (mainly spermine), total creatine (Cr) and citrate (Cit). Elevated Cho, and reduced PA and Cit are recognized as markers for prostate malignancy.

Most studies that performed 3D MRSI examinations of the prostate, used an endorectal coil in combination with a phased-array surface coil. A typical nominal voxel size in these studies ranged between 5x5x5 mm^3 and 7x7x7 mm^3 [18,19]. One major disadvantage of 3D MRSI is the necessity to use an inflatable endorectal receiver coil to achieve sufficient signal-to-noise ratio (SNR) within a clinically acceptable scanning time. However, endorectal coils cannot be used during RT as well as during the first 1-2 months after RT. The endorectal coil is contraindicated in patients with rectal bleeding, severe hemorrhoids, painful rectal fissures, Crohn's disease, and ulcerative colitis. Some patients are also reluctant to repeat the examination with an endorectal coil because insertion of the coil into rectum is an unpleasant or painful procedure [5,19].

The main goal of this study was assessment of prostate metabolic activity using single-voxel MRS and evaluation of ADC variations before, during and three months after the completion of BT and/or EBRT. The second aim was to investigate both methods in assessing the response of prostate tissues to RT.

Materials and methods

Patients

Seven patients with biopsy-proven localized T1cN0M0 intermediate-risk PCa participated in this study (Table 1). Two patients (nr 1 and 2) received combined BT and EBRT and five were treated by EBRT only. Three patients received short-course neo-adjuvant androgen-deprivation therapy (ADT) before the start of therapy. Patients nr 1 and 7 were treated by bicalutamide and finasteride and patient nr 3 had received a combination of bicalutamide and tamoxifen. None of the other patients (nr 2,4,5, 6) had received any other treatment for PCa prior to therapy. The local ethical committee approved this study and written informed consent was obtained from all participants before commencing the study.

Radiotherapy

Brachytherapy was performed under local anesthesia. Transrectal ultrasound imaging was used to guide positioning of the BT sources in prostate. Two high-dose rate (Ir-192) BT sessions were performed fortnightly delivering a dose of 20 Gy (10 Gy/fraction) to the whole prostate and the base of seminal vesicles. Linac-based conventional EBRT followed a day after BT delivering a dose of 50 Gy in 25 fractions. External RT was delivered with volumetric modulated arc therapy (6 MV) in patients nr 1 and 2 resulting in a total delivered nominal dose of 70 Gy. Patients nr 3-7 were treated with EBRT only, receiving a ultra hypo-fractionated regimen of 42.7 Gy in 7 fractions [20] using 1.5T MR-Linac (Unity, Elekta AB, Stockholm, Sweden). Here, RT was delivered with step-and-shoot intensity modulated technique (IMRT, 7 MV) under daily MR imaging. Target and organ-at-risk structures were adapted to the daily inner anatomy as observed in the MR images and a new RT plan was optimized and delivered at each fraction according to an MR-guided adaptive RT workflow for Unity [21].

Data acquisition

MR examinations of all patients were performed on a 3T clinical scanner (Elition, Philips Healthcare, Best, the Netherlands). MRI acquisitions were performed about one week before the treatment (BT or EBRT), after first BT, twice during EBRT, and about 3 months after RT. A 32-channel receiver phased-array surface coil was used for imaging and spectroscopy. Sagittal, coronal, and axial T_2-weighted turbo spin echo images were acquired to guide positioning of the spectroscopic voxel position (TR/TE=3758/110 ms; field of view (FOV)=160x160 mm^2; acquisition matrix=200 x157; slice thickness=3 mm; SENSE factor=1.3; bandwidth/pixel=220.1 Hz; number of signal averages (NSA)=1). Diffusion-weighted images were acquired by single-shot spin-echo with an echo-planar readout (SE-EPI) sequence (TR/TE=3500/68 ms; FOV =

160x160 mm^2; acquisition matrix=(64 x 64); slice thickness=3 mm; slice gap=0 mm; SENSE factor=3; NSA=3; EPI bandwidth=1985 Hz; spectrally selective attenuated inversion recovery (SPAIR) fat suppression). Diffusion gradients were applied in three directions using a range of b-values (b=0,100,250,400,600 s/mm^2). Axial ADC maps were then computed from the diffusion data using the vendor software which employed a mono-exponential fit.

Single-voxel spectroscopy was performed with the point-resolved spectroscopy (PRESS) sequence (TR/TE=1500/140 ms; phase cycling=16). Sixteen non-water suppressed acquisitions were followed by 384 water-suppressed scans. Magnetic field homogeneity was improved by iterative first-order shimming. Water suppression was performed by band selective pre-pulses and by band-selective inversion with gradient dephasing (BASING) pulses [22]. Fat suppression was achieved by a frequency-selective inversion recovery pre-pulse. The largest possible voxel was placed inside the prostate while minimizing inclusion of periprostatic fat. For all patients, the shortest distance between the acquisition voxel and eventual rectal air was roughly 10 mm. The total MRI and MRS examination time including patient positioning was approximately 35-40 minutes.

Data analysis

Since the entire prostate volume was treated by RT, the aim of data analysis was to characterize radiation-induced changes in the largest possible prostate volume. The five axial slices placed at the center of prostate were used for evaluation of the ADC values. We assumed that the slice positions were approximately the same in the measurements before, during, and three months after the end of the therapy. Regions of interest (ROIs) were drawn manually and encompassed the whole peripheral zone and the central gland. Great attention was paid to exclude the neurovascular bundle around the prostate and urethra (if visible). ADC values were quantified in all five slices and the average value was calculated. Benign and malign prostate tissues were not evaluated separately.

All spectra were processed in LCModel v. 6.3-1K [23]. Unlike other spectrum processing software, LCModel does not utilize apodization of the time domain signal to improve SNR. LCModel utilizes an algorithm that fits prostate spectrum with simulated Cho, PA, Cr, and Cit spectral lines as the prior knowledge. Reliability of the spectral line fit is given by a standard deviation (Cramér-Rao lower bound) expressed in percent of the estimated concentrations. A CRLB<20% is usually used as a criterion that the spectral line fit is of acceptable reliability. The metabolite is practically undetectable if CRLB>40%. Based on LCModel vendor recommendation, a SNR>3 was used as a criterion of prostate spectrum acceptance. Total Cho, PA, total Cr, and Cit quadruplet were fitted in LCModel. Spectral intensity ratios Cho/(PA+Cr) were evaluated instead of Cho/Cr because separation of PA and Cr spectral lines was unreliable. Since Cit intensity can potentially decrease to the noise level at the end of therapy, the Cit/(Cho+PA+Cr) spectral intensity ratio was evaluated instead of (Cho+PA+Cr)/Cit. Furthermore, radiation therapy-induced changes of Cho spectral line is more difficult to evaluate. Since PA decreases during the therapy and Cr cannot be fitted accurately due to overlapping with PA line, Cho/Cr ratio cannot be quantified reliably. Also Cho to unsuppressed water line cannot be quantified reliably because prostate water concentration is not constant during the therapy. To overcome these difficulties, the SNR of the Cho spectral line was used as a measure of Cho intensity. To justify such assumption, it was assumed that the distance between the surface coil and prostate was almost constant for all measurements and that the voxel volume was unchanged. The former was possible to achieve with reasonable accuracy by placing the center of the surface coil directly above the prostate and also the fact that patient shape did not change during the therapy.

Statistics

The reported values are given as the mean ±1 SD.

Results

Single-voxel spectroscopy was succesfully performed for all patients. All acquired spectra had a SNR>3 (range 4-15). The mean voxel size and water linewidth after shimming were 18.1±5.5 cm^3, and 16.5±3.9 Hz, respectively. A typical voxel position in the prostate is shown in Figure 1. The processed spectrum of patient nr 1 before therapy is shown in Figure 2. It can be seen from Figure 2 that despite having a very good spectrum quality (SNR = 6), Cr was fitted unreliably (CRLB>40%). However, the sum of PA+Cr spectral line fit was reliable (CRLB=10%). The spectra of patients nr 1 and 2 treated with BT and EBRT are shown in Figure 3. The intensities of PA and Cit are noticeably decreased after the second BT (Figure 3c). Spectral intensity of Cit dropped almost to the noise level three months after the end of EBRT for both of the patients (Figure 3d). At the same time, PSA levels dropped from 2,1 and 3,3 ng/mL prior to therapy to 0.5 and 0,9 ng/mL, respectively at three months follow-up (Table 1) indicating a relationship between the decreased Cit intensity and a very good initial biochemical response of prostate to the combined treatment. Spectra of the patients treated only by EBRT are shown in Figure 4. These spectra reveal gradual decrease of PA and Cit intensities. Compared to the initial values shown in Figure 4a, the levels of Cit decreased considerably three months after the end of EBRT (Figure 4d). This together with declining PSA levels (Table 1) reveal an apparent biochemical response to therapy. The exception was patient nr 4, whose spectum is shown in Figure 4d, with a relatively high Cit intensity three months after the end of EBRT. This demonstrates the worst metabolic response to the EBRT in our patient population. Interestingly, the same patient had a relatively high PSA values at 9 months standard follow-up (Figure 5). Mean Cho/(PA+Cr) spectral intensity ratio of all patients before therapy was 0.59±0.36 increasing to 1.17±0.5 three months after the end of therapy. Mean Cit/(Cho+PA+Cr) ratio of all patients with the exception of patient nr 4 was 0.32±0.13 three months after the end of therapy. The excluded patient nr 4 had a ratio of 0.79. This strengthens our belief that a good response to therapy might be quantitavely expressed by the spectral intensity ratio Cit/(Cho+PA+Cr)<0.32±0.13. SNR of the Cho spectral line was evaluated as a measure of Cho concentration. The condition of constant voxel volume during all measurements was met in patients nr 1,2,3,5, and 7. SNR difference of Cho lines between the first irradiations (Figures 3b and 4b) and three months after the end of the therapy (Figures 3d and 4d) was in the range ±1, while mean Cho SNR of the patients during the same period was 5.2±0.9 (range 4-7).

PSA values of the patients before the start of androgen-deprivation therapy (ADT) or before the start of RT, respectively. PSA values where evaluated 3,6 months, and 9-12 months after the EBRT.

The time course of prostate ADC values for all patients is shown in Figure 6. The first measurements were performed one week (day-6) before the start of therapy and the last measurements were performed ~3 months after the end of therapy. As indicated in Figure 6, therapy started on day 1. It is inferred from Fig 6 that BT resulted in a fast decrease of ADC values followed by an increase. On the contrary, the ADC values of the patients treated only by EBRT increased during the therapy (Figure 6b). The only exception was patient nr 4 where ADC values did not change during the therapy taking into consideration standard deviations. The increase of ADC values three months after the end of therapy compared to the values before therapy was insignificant ($p>0.05$).

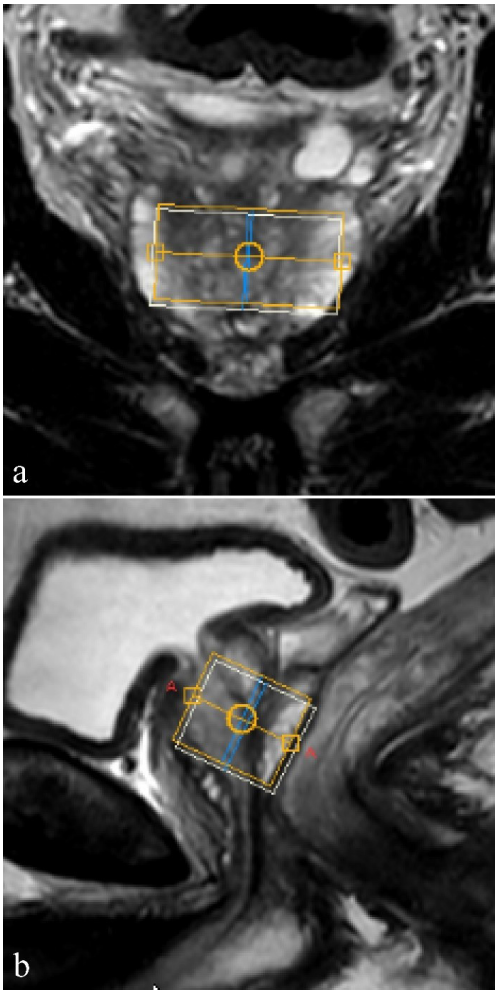

Figure 1: Volume of interest position. A typical voxel position in the prostate in (a) coronal and (b) sagittal slice. Citrate and choline voxels are depicted by yellow and white lines respectively.

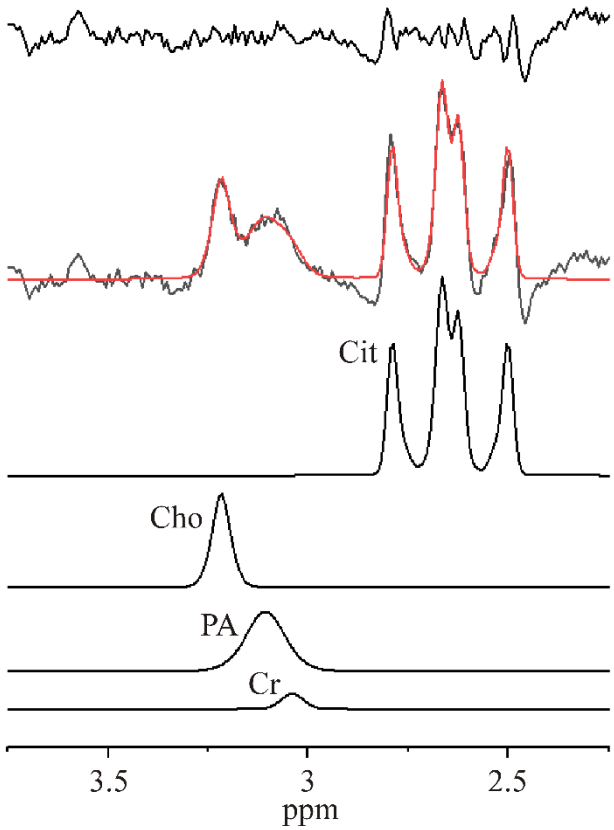

Figure 2: Spectrum processing. LCModel processed spectrum of patient nr 1 before therapy. The solid (red) line overlaid on the measured spectrum indicates fit. Bottom: fitted metabolites of citrate (Cit), choline (Cho), polyamines (PA), and creatine (Cr). Top: residual from the fit.

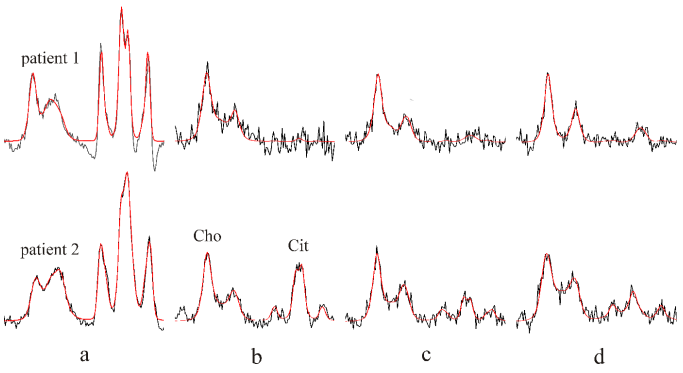

Figure 3: Prostate spectra of the patients treated with brachytherapy (BT) and external beam radiopherapy (EBRT). The solid (red) line overlaid on the measured spectrum indicates fit. **(a)** One week before therapy, **(b)** after the first BT, **(c)** after the second BT and EBRT (four fractions of EBRT for patient nr 1) and (seven fractions of EBRT for patient nr 2), **(d)** three months after the end of EBRT. Choline (Cho) and citrate (Cit) spectral lines.

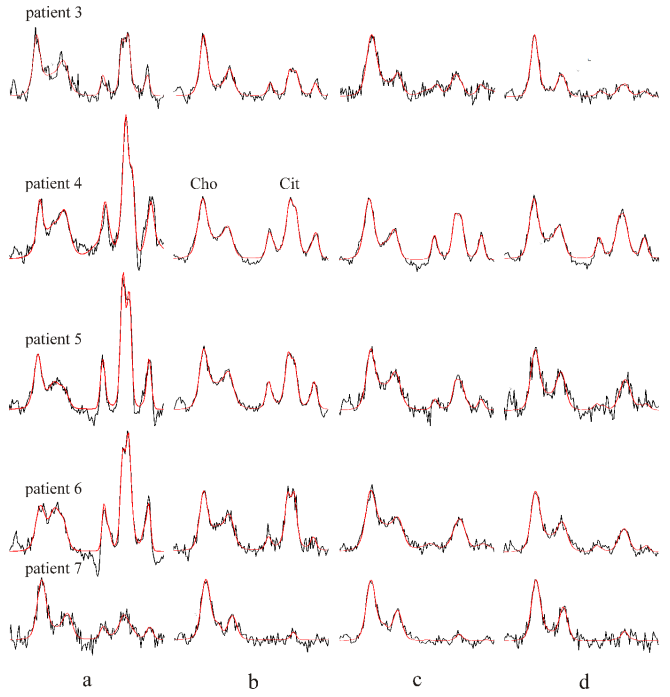

Figure 4: Prostate spectra of patients treated with external beam radiotherapy (EBRT) only. The solid (red) line overlaid on the measured spectrum indicates fit. **(a)** One week before therapy, **(b)** immediately after fourth ±1 fraction of EBRT, **(c)** at the end of EBRT, **(d)** 3 months after the end of therapy. Choline (Cho) and citrate (Cit) spectral lines.

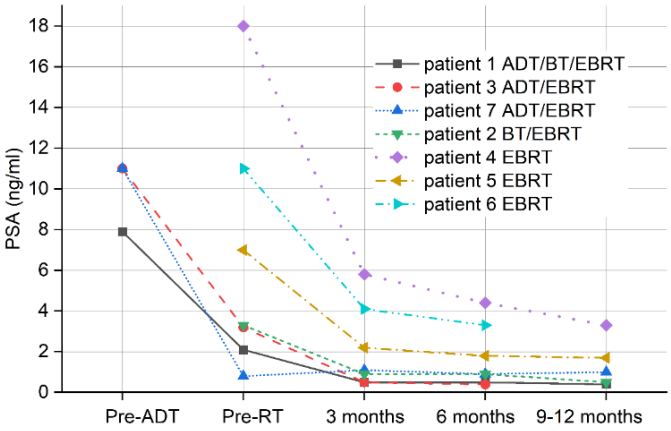

Figure 5: Biochemical response of prostate to radiotherapy (RT) over the time measured by serum prostate-specific antigen (PSA) levels. Patients reveived either brachytherapy (BT) combined with external bean radiotherapy (EBRT) or only EBRT.

Discussion

Radiation-induced metabolic response in prostate after RT has attracted scientific attentions to explore its predictive value in treatment of PCa. In this work, surveillance of prostate metabolic changes for two RT strategies (EBRT + BT vs EBRT only) was performed pre, per- and post-treatment using single-voxel spectroscopy. To the best of our knowledge, this is the first report of its kind where RT was monitored by single-voxel spectroscopy without the need for the use of an endorectal receiver coil. High quality spectra were acquired in a short measurement time and

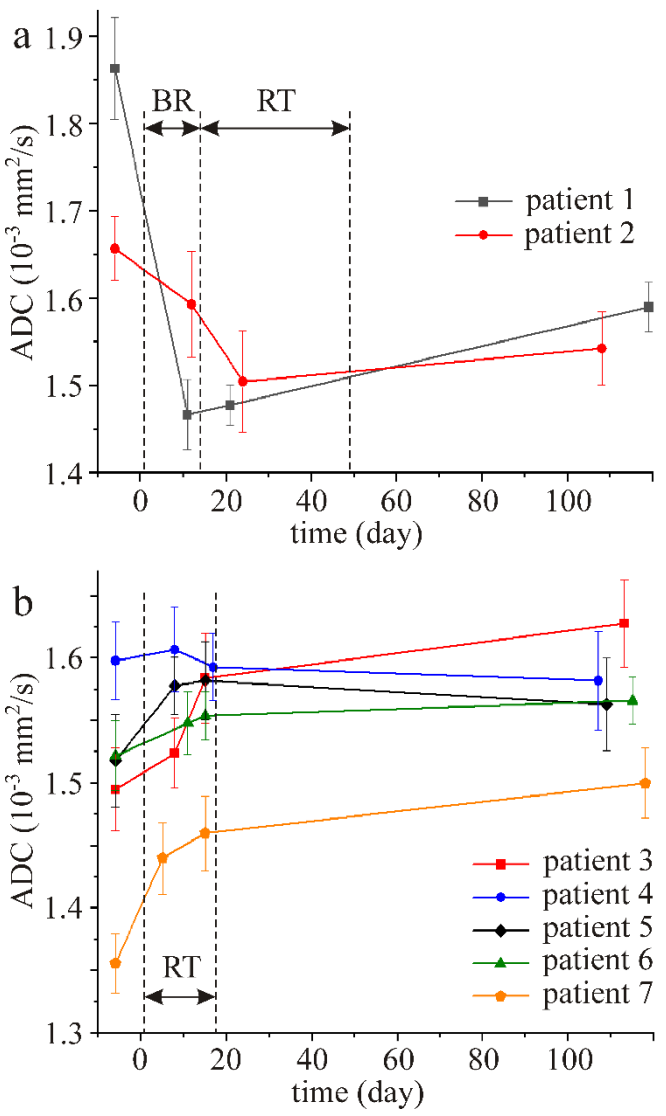

Figure 6: Time course of the prostate ADC values. The first measurements were performed one week (day 6) before beginning of the therapy. The last measurements were done ~3 months after the end of therapy. Therapy started on day 1. **(a)** Patients treated by brachy- (BR) and external beam radiotherapy (EBRT), **(b)** patients treated only by EBRT. Dashed vertical lines depict periods of BR and EBRT.

it is our belief that omitting the endorectal coil from the workflow, was the only acceptable alternative for the recruitment of patients with PCa undergoing RT.

Previous prostate MR spectra of patients treated by EBRT or ADT were performed exclusively with 3D MRSI techniques [3,5, 15-18]. The examinations required an endorectal coil in combination with a phased-array surface coil and their main purpose was detection of residual or recurrent PCa after therapy [3,5,8, 13] and verification of successful treatment by identifying metabolic atrophy. However, all reported spectra from small 3D MRSI voxels had poor SNR. Therefore, noise suppression was an inevitable step in spectrum processing, which resulted in a decrease in spectral resolution. In some studies, Cho, PA and Cr spectral lines were indistinguishable [5,15,17].

The term “metabolic atrophy” (MA) was first introduced by Mueller-Lisse et al in 2001 [15]. The authors identified the pres-

Table 1: Patients' characteristics.

Patient nr	Age (years)	Gleason score	Dominant tumor size (cm)	Radiation dose (Gy)	Treatment	PSA Pre-ADT	PSA Pre-RT	PSA 3 months after RT
1	60	3+4	1	70	ADT/BT/ EBRT	7.9	2.1	0.5
2	57	4+3	1	70	BT/EBRT		3.3	0.9
3	76	4+3	2.3	42.7	ADT/EBRT	11.0	3.2	0.5
4	74	4+3	0.9	42.7	EBRT		18	5.8
5	75	4+3	1.2	42.7	EBRT		7.0	2.2
6	75	4+3	1.1	42.7	EBRT		11.0	4.1
7	67	3+4	0.8	42.7	ADT/EBRT	11.0	0.8	1.1

ADT: Androgen deprivation therapy; BT: Brachytherapy; EBRT: External beam radiotherapy; PSA levels in ng/ml.

ence of MA in voxels where (Cho+Cit) intensity (peak area) ratio to noise was less than 5. They proposed that complete MA was achieved when spectral intensities of all detectable metabolites were less than 5 SD of the noise level. The definition of MA was further enhanced by Pickett et al [5] and Valentini et al [6] where the occurrence of MA was defined as the (Cho+PA+Cr+Cit) intensity ratio to noise was less than 5. The very last MA definition was proposed by Panebianco et al [17] as the spectral intensity ratio (Cho+PA+Cr)/Cit<0.2. There are drawbacks associated with all definitions. SNR is an unreliable reference to the spectral intensities because it is influenced by additional factors. SNR is dependent on the distance between surface coil and prostate, which in turn depends on patient shape and size. Other critical factors are voxel size, number of signal averages and TR. In addition, SNR is first suppressed in vendor-dependent spectrum processing and then used as a noise reference [5,6,15]. The definition of Panebianco et al. [17] is also problematic because Cit intensity can be very low or undetectable at the end of the RT or indeed a few months after.

PA and Cit are the most sensitive metabolites to RT. Both metabiltes are produced by epithelial cells and stored in the luminal compartments. A high level of PA and Cit intensities reveal an active prostate metabolism. PA and Cit decrease in malign prostate tissues due to invasion of secretory ducts by cancer cells and also by decrease of luminal volume. Further decrease of PA and Cit is caused by reduced production of spermine by cancer cells and by Cit oxidation due to the neoplastic cells failure to accumulate zinc [24,25]. Our results have demonstrated that PA and Cit intensities were reduced very fast due to irradiation damage of healthy secretory epithelial cells which go first to apoptosis. The consequence was an increase of Cho/(PA+Cr) ratio and decrease of Cit/(Cho+PA+Cr) spectral intensity ratio.

Previous studies reported radiotherapy-induced decrease of Cho (cell membrane constituent) and Cr intensities in addition to the much faster reduction of PA and Cit spectral lines [5,6,15-17]. To verify the decrease of Cho spectral intensity, we used SNR of the Cho spectral line as a measure of the Cho content. For each patient, only minimal differences were found between Cho SNR after the first irradiation fractions (Figures 3b and 4b) and SNR three months after the end of therapy (Figures 3d and 4d). In other words, RT induced changes in Cho concetration were very small (if any). One can therefore conclude that the reduction of Cit intensity close to the noise level seems to be the most reliable measure for identification of metabolic atrophy and response to therapy. In our patient population, complete metabolic atrophy, which is defined as a loss of all prostate spectral intensities, was not reached. We believe that complete metabolic atrophy is an unattainable goal in current standard radiation treatment, which is also reflected by the PSA levels after RT (Figure 5).

ADC time course of prostate treated by a combined BT and EBRT (Figure 6a) was qualitatively different compared to the ADC time course of the patients treated only by a ultra-hypo-fractionated EBRT regimen (Figure 6b). Brachytherapy caused rapid decrease of ADC values. Restricted diffusion of the free water molecules was most likely caused by decrease of extracellular space due to hemorrhage and inflammatory swelling of cells associated with BT. On the contrary, ADC values increased during EBRT and were higher three months after the end of the therapy compared to the values before therapy (Figure 6b). This increase in ADC in both PCa and benign tissues was also observed in previous studies [12,26-28]. Post-radiation ADC increase is usually explained by changes characterized by lower cellularity associated with glandular atrophy and fibrosis. In our studied population, surveillance of both metabolic and ADC changes during and after RT in patient 4 revealed a somewhat aberrant profile. Interestingly, the long term declining of his PSA levels were relatively slow reaching to 3,3 ng/ml at 9 months follow-up (Figure 5). In the study of 18 patients with PCa who received non-ADT EBRT, Chow et al. [29] found that all the patients without biochemical recurrence had a 9 months PSA levels <1.0 ng/ml. Hence, longer surveillance of this patient should reveal the predictive value of the observed metabolic changes of the prostate in this particular case.

The main limitation of the present work is the small number of patients. We had originally intended to examine five patients treated by combined BT and EBRT and five patients treated only by EBRT but our efforts were hampered by the COVID-19 pandemic. Therefore, only two patients with combined BT and EBRT were available for our evaluations. Further limitation of this work is that the metabolic profile and ADC values were analysed for the whole prostatic tissue and not specifically the tumour lesions or benign tissue. However, we believe that reactions in the whole prostate can be used as a surrogate for metabolic changes in the tumour tissues as well. Our last measurements were performed three months after the end of the therapy, which clinically is too short to verify a long-term response to RT. Thus, results of this study require confirmation in a larger cohort of patients with a longer (2-3 years) follow-up period.

Conclusion

Single-voxel spectroscopy is a useful tool for monitoring metabolic changes in prostate treated with BT and/or EBRT. Our results suggest that a biochemical response to RT of intermediate-risk PCa, might be characterized by low Cit intensity and an increase in ADC after the treatment. On the other hand, higher Cit intensity and negligible changes of ADC values after the end of therapy compared to the values before therapy suggest poor biochemical response to the treatment. Spectroscopic data of metabolic activity may provide important predictive information following RT. Future work is intended to investigate the role of single-voxel spectroscopy in assessing the response of prostate to RT in a larger cohort of patients.

Declarations

Conflict of interest: Authors declare no conflict of interest.

Funding: This study was supported by Foundation of Department of Oncology, University Hospital, Uppsala, Sweden.

Acknowledgement: We would like to thank the coordinator personnel and oncologist colleagues for their involvement in booking, recruiting and follow-up of the patients.

References

1. Gwede CK, Pow-Sang J, Seigne J, Heysek R, Helal M, Shade K, et al. Treatment decision-making strategies and influences in patients with localized prostate carcinoma. Cancer. 2005; 104: 1381-1390.
2. Vulto JC, Lybeert ML, Louwman MW, Poortmans PM, Coebergh JW. Population-based study of trends and variations in radiotherapy as a part of primary treatment of cancer in the southern Netherlands between 1988 and 2006, with an emphasis on breast and rectal cancer. Int J Radiat Oncol Biol Phys. 2009; 74: 464-471.
3. Albertsen PC, Hanley JA, Penson DF, Barrows G, Fine J. 13-year outcomes following treatment for clinically localized prostate cancer in a population based cohort. J Urol. 2007; 177: 932-936.
4. Wilt TJ, Thompson IM. Clinically localised prostate cancer. BMJ. 2006; 333: 1102-1106.
5. Pickett B, Kurhanewicz J, Coakley F, Shinohara K, Fein B, Roach M. Use of MRI and spectroscopy in evaluation of external beam radiotherapy for prostate cancer. Int J Radiation Oncology Biol Phys. 2004; 60: 1047-1055.
6. Valentini AL, Benedetta G, D'Agostino GR, Mattiucci G, Clementi V, Di Molfetta IV. Locally advanced prostate cancer: Three-dimensional magnetic resonance spectroscopy to monitor prostate response to therapy. Int J Radiation Oncology Biol Phys. 2012; 84: 719-724.
7. Song I, Kim CK, Park BK, Park W. Assessment of response to radiotherapy for prostate cancer: Value of diffusion-weighted MRI at 3 T. Am J Roentgenol. 2010; 194: W477-482.
8. Kirilova A, Damyanovich A, Crook J, Jezioranski J, Wallace K, Pintilie M. 3D MR-spectroscopic imaging assessment of metabolic activity in the prostate during the PSA "bounce" following 125Iodine brachytherapy. Int J Radiation Oncology Biol Phys. 2011; 79: 371-378.
9. Sandhu S, Moore CM, Chiong E, Beltran H, Bristow RG, Williams SG. Prostate cancer. Lancet. 2021; 398: 1075-1090.
10. Kishan AU. PSA bounce, prognosis, and clues to the radiation response. Prostate Cancer and Prostatic Diseases. 2021; 24: 937–938.
11. Kuban DA, Thames HD, Levy LB, E, Horwitz EM, Kupelian PA, Martinez AA, et al. Long-term multi-institutional analysis of stage T1-T2 prostate cancer treated with radiotherapy in the PSA era. Int J Radiation Oncology Biol Phys. 2003; 57: 915-928.
12. Kim CK, Park BK, Lee HM. Prediction of locally recurrent prostate cancer after radiation therapy: Incremental value of 3T diffusion-weighted MRI. J Magn Reson Imag. 2009; 29: 391-397.
13. Westphalen AC, Coakley FV, Roach M, McCulloch CE, Kurhanewicz J. Locally recurrent prostate cancer after external beam radiation therapy: Diagnostic performance of 1.5-T endorectal MR imaging and MR spectroscopic imaging for detection. Radiology. 2010; 256: 485-492.
14. Morgan VA, Riches SF, Giles S, Dearnaley D, deSouza NM. Diffusion-weighted MRI for locally recurrent prostate cancer after external beam radiotherapy. Am J Roentgenol. 2012; 198: 596-602.
15. Mueller-Lisse UG, Swanson MG, Vigneron DB, Hricak H, Bessette A, Males RG, et al. Time-dependent effects of hormone-deprivation therapy on prostate metabolism as detected by combined magnetic resonance imaging and 3D magnetic resonance spectroscopic imaging. Magn Reson Med. 2001; 46:49-57.
16. Mueller-Lisse UG, Swanson MG, Vigneron DB, Kurhanewicz J. Magnetic resonance spectroscopy in patients with locally confined prostate cancer: Association of prostatic citrate and metabolic atrophy with time on hormone deprivation therapy, PSA level, and biopsy Gleason score. Eur Radiol. 2007; 17: 371-378.
17. Panebianco V, Barchetti F, Musio D, Forte V, Pace A, De Felice F, et al. Metabolic atrophy and 3-T 1H-magnetic resonance spectroscopy correlation after radiation therapy for prostate cancer. BJU Int. 2014; 114: 852-859.
18. Kobus T, Vos PC, Hambrock T, De Rooij M, Hulsbergen-Van de Kaa CA, Barentsz JO, et al. Prostate cancer aggressiveness: In vivo assessment of MR spectroscopy and diffusion-weighted imaging at 3 T. Radiology. 2012; 265: 457-467.
19. Weis J, von Below C, Tolf A, Ortiz-Nieto F, Wassberg C, Häggman M, et al. Quantification of metabolite concentrations in benign and malignant prostate tissues using 3D proton MR spectroscopic imaging. J Magn Reson Imaging. 2017; 45: 1232-1240.
20. Widmark A, Gunnlaugsson A, Beckman L, Thellenberg-Karlsson C, Hoyer M, Lagerlund M, et al. Ultra-hypofractionated versus conven- tionally fractionated radiotherapy for prostate cancer: 5-year outcomes of the HYPO-RT-PC randomised, non-inferiority, phase 3 trial. Lancet. 2019; 394: 385-395.
21. Winkel D, Bol GH, Kroon PS, van Asselen B, Hackett SS, Werensteijn-Honingh AM, et al. Adaptive radiotherapy: The Elekta Unity MR-linac concept. Clin Transl Radiation Oncology. 2019; 18: 54-59.
22. Star Lack J, Nelson SJ, Kurhanewicz J, Huang LR, Vigneron DB. Improved water and lipid suppression for 3D PRESS CSI using RF band selective inversion with gradient dephasing (BASING). Magn Reson Med. 1997; 38: 311-321.
23. Provencher SW. Estimation of metabolite concentrations from localized in vivo proton NMR spectra. Magn Reson Med. 1993; 30:672-679.

24. Smith RC, Litwin MS, Lu Y, Zetter BR. Identification of an endogenous inhibitor of prostatic carcinoma cell growth. Nat Med. 1995; 1: 1040-1045.

25. Micielska ME, Patel A, Rizaner N, Mazurek MP, Keun H, Patel A, et al. Citrate transport and metabolism in mammalian cells. BioEssays. 2009; 31: 10-20.

26. Sato C, Naganawa S, Nakamura T, Kumada H, Miura S, Takizawa O, et al. Differentiation of non-cancerous tissue and cancer lesions by apparent diffusion coefficient values in transition and peripheral zones of the prostate. J Magn Reson Imaging. 2005; 21: 258-262.

27. Westphalen AC, Galen DR, Vinh PP, Sotto C, Vigneron DB, Kurhanewicz J. Multiparametric 3T endorectal MRI after external beam radiation therapy for prostate cancer. J Magn Reson Imaging. 2012; 36: 430-437.

28. Takayama Y, Kishimoto R, Hanaoka S, Nonaka H, Kandatsu S, Tsui H, et al. ADC value and diffusion tensor imaging of prostate cancer: changes in carbon-ion radiotherapy. J Magn Reson Imaging. 2008; 27: 1331-1335.

29. Chow PM, Chiang IN, Cheng JCH, Chiang BJ, Pu YS, Huang CY. Pretreatment prostate specific antigen (PSA) and 2-year PSA dynamics: Early predictors of prostate cancer prognosis with external radiation therapy. Urological Science. 2013; 24: 120-123.